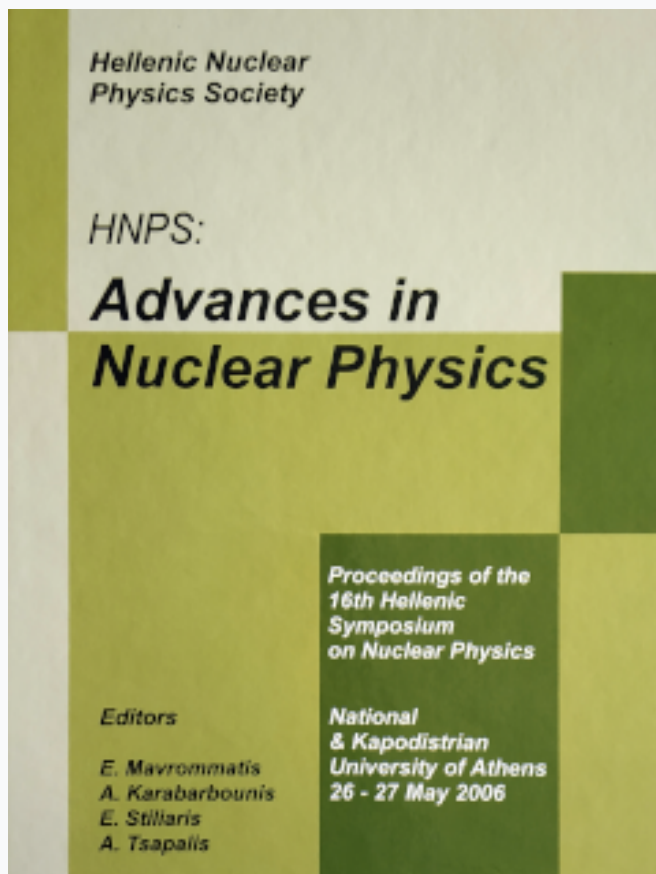


## HNPS Advances in Nuclear Physics

Vol 15 (2006)

HNPS2006



### Position and Energy Resolution of a $\gamma$ -Camera based on a Position Sensitive Photomultiplier Tube

A. Polychronopoulou, D. Thanasas, N. Giokaris, A. Karabarounis, D. Maintas, C. N. Papanicolas, E. Stiliaris

doi: [10.12681/hnps.2635](https://doi.org/10.12681/hnps.2635)

#### To cite this article:

Polychronopoulou, A., Thanasas, D., Giokaris, N., Karabarounis, A., Maintas, D., Papanicolas, C. N., & Stiliaris, E. (2020). Position and Energy Resolution of a  $\gamma$ -Camera based on a Position Sensitive Photomultiplier Tube. *HNPS Advances in Nuclear Physics*, 15, 172–179. <https://doi.org/10.12681/hnps.2635>

## Position and Energy Resolution of a $\gamma$ -Camera based on a Position Sensitive Photomultiplier Tube

A. Polychronopoulou <sup>a</sup>, D. Thanasas <sup>a</sup>, N. Giokaris <sup>ab</sup>, A. Karabarounis <sup>ab</sup>,  
D. Maintas <sup>c</sup>, C.N. Papanicolas<sup>ab</sup> and E. Stiliaris<sup>ab\*</sup>

<sup>a</sup>Physics Department, National and Kapodistrian University of Athens

<sup>b</sup>Institute of Accelerating Systems and Applications (IASA)

<sup>c</sup>Institute of Isotopic Studies, Athens

Studies of the spatial- and energy-resolution of a small field, high resolution  $\gamma$ -Camera system currently being developed in our laboratory are presented here. The system is based on a cylindrical Position Sensitive Photo-Multiplier Tube (HAMAMATSU R2486) with 32 crossed-wired anodes, arranged in two orthogonal groups. The anode outputs are connected to a resistive current divider network and after pre-amplification are guided to a local digitizing system. A PCI-Analog to Digital Converter card with a maximum sampling rate of 20 MHz and the rest of the Data Acquisition System is controlled by software running on the LabVIEW<sup>®</sup> environment. Position and induced charge of the incident light pulses can be easily reconstructed through a variety of offline algorithms.

In the first part of this study the intrinsic response of the PMT and especially its energy and position resolution is presented. The experimental procedure utilizes the controlled pulse light output of a LED guided through fiber glass directly to the PMT's entrance. The accumulated charge distribution and charge spread as a function of the incident number of photons is studied. In the second part, the response of the integrated  $\gamma$ -Camera system after the application of typical scintillation crystals for <sup>99</sup>Tc radioactive phantoms is measured and analyzed.

### 1. Introduction

In many molecular imaging applications using gamma emitters it is often necessary to obtain information about the energy and spatial distribution of the radiotracer administered to a patient for clinical *in vivo* explorations. Classical Single Photon Emission Computed Tomography (SPECT) techniques require high resolution in the planar images obtained with position sensitive detection systems. This is the reason why the Anger  $\gamma$ -Camera [1] is being continuously developed and has become a standard choice for clinical applications [2]–[7].

The principle of operation of a  $\gamma$ -Camera is based on the use of a scintillation material that interacts with the  $\gamma$ -rays emitted from the radiotracer and the detection of the

---

\*Corresponding author: stiliaris@phys.uoa.gr

generated light pulses. In order to retain the position information a collimator is used in front of the scintillation crystal allowing only the  $\gamma$ - rays parallel to the camera's main axis to enter the system.

It is widely recognized that SPECT devices used in clinical research must offer both excellent spatial resolution and a high level of detection efficiency. We have designed and performed basic feasibility test [8,9] with a parallel-hole small field  $\gamma$ -imaging system based on a commercially available Position Sensitive PhotoMultiplier Tube (PSPMT) and PCI electronics, with the goal of submillimeter spatial resolution and high detection efficiency. The major part of the work reported here is a first attempt to define with high accuracy the limiting factors of the system and it is dedicated to the study of the intrinsic response of the photomultiplier tube, which unavoidably sets the limits for both spatial and energy resolution.

## 2. The $\gamma$ -Camera System

The main components of the  $\gamma$ -Camera system are a lead parallel-hole collimator, a 4 mm thick pixelated CsI(Tl) scintillator and the Position Sensitive PhotoMultiplier Tube (PSPMT), model HAMAMATSU R2486 [10]. The 3" diameter cylindrical envelope photomultiplier tube is composed of a Bialkali photocathode, a 12 stage coarse mesh dynode structure and 32 crossed-wired anodes arranged into two orthogonal groups X and Y, as shown in Figure 1.

The anode output wires are connected to a resistive current divider network so that the number of the readout signals is reduced to four analog signals ( $X_A, X_B, Y_C, Y_D$ ). Both the energy and the position of the incident photons can be reconstructed from these four signals. The total energy of the photon is proportional to the total charge accumulated and the position at each axis can be reconstructed from the normalized difference of the two corresponding signals, following the relations:

$$X - Position : \quad X \sim (X_A - X_B) / (X_A + X_B) \quad (1)$$

$$Y - Position : \quad Y \sim (Y_C - Y_D) / (Y_C + Y_D) \quad (2)$$

$$Energy : \quad Q \sim (X_A + X_B) + (Y_C + Y_D) \quad (3)$$

The readout system comprises a fast analog to digital converter (ADC) on a PCI card, model PCI-9812 ADLink [11], with four single ended input channels that lead to four A/D converters simultaneously running with a maximum sampling rate of 20 MHz. Other important features of this card are the 12 bit analog input resolution, the ability to use bipolar input signals and the option of an external trigger mode. The whole digitizing and data acquisition system is controlled by software developed on the LabVIEW® environment.

Each one of the analog signals can be digitized into an external adjusted number of points providing thus the ability to find the pulse height. Since the pre-amplified charge signals are negative, the minimum of the sampled points determines in a first approach the height of the signal. The introduced signal error  $\Delta S$  by this simplified method is strongly correlated with the sampling rate  $f$  and the steepness of the signal  $[dS/dt]_0$  near

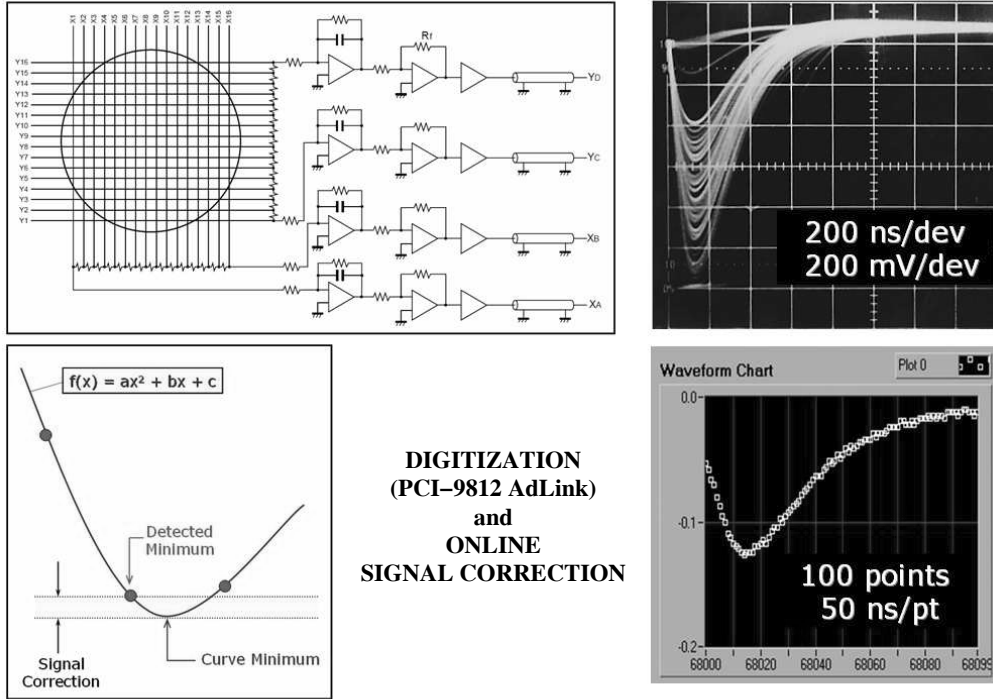


Figure 1. *Upper part:* Wiring scheme for the 16+16 anode signals of the HAMAMATSU R2486 Photomultiplier tube through the resistive chain and the four charge preamplifiers. The analog signal output for a typical CsI(Tl) scintillator is shown in the right figure. *Lower part:* Signal sampling after digitization with the PCI-9812 card and the principle of the 2<sup>nd</sup> order correction algorithm for the location of the minimum.

the minimum; in the worst case it is given by the estimate:

$$\Delta S = \frac{1}{2} \left[ \frac{dS}{dt} \right]_0 \frac{1}{f} \quad (4)$$

For the maximum of the sampling rate (20 MHz which corresponds to 50 ns/point) and for a typical signal obtained with the 4 mm thick CsI(Tl) scintillator (see Figure 1) the estimated relative error in the signal averages  $\sim 2 - 3\%$ . In order to eliminate this experimental uncertainty an optimized method based on a curve fit has been introduced. According to this method, the location of the signal minimum  $S_{cor}$  is extracted from the second order polynomial function fitted to the three digitized points by taking in account also the other two (left-right) neighboring measures (Figure 1). The relative difference of the pulse height  $\Delta S_{rel}$  obtained from the above method

$$\Delta S_{rel} = (S_{min} - S_{cor})/S_{cor} \quad (5)$$

can be used as a convergence criterion for higher order corrections. It is proved that the method is practically saturated by the second order correction and any improvement by

higher order fits will be overlaid by the signal noise. The second order correction algorithm has been online implemented in the DAQ-system and is used in all measurements described below.

### 3. Experimental Setup

#### 3.1. Intrinsic Response Study

In the following the experimental setup is presented used to study the intrinsic response of the PSPMT against any possible deviations from linearity. Extensive measurements were performed in order to define and characterize its energy and spatial resolution before the coupling of any scintillating material. The experimental setup used here is the same as in previous measurements [8] but with some mechanical improvements. A green LED driven by a pulse generator (CAMAC model BiRa) with a 1 mm in diameter optical fiber illuminates the photosensitive entrance window of the PSPMT. A grid plate with 21 equidistant holes was placed in front of the PSPMT window so that the optical fiber can be fixed in each one of the holes in well predefined relative distances. In Figure 2 the geometry of the grid is presented together with the reconstructed position from data obtained for a fixed pulse duration and high voltage operation.

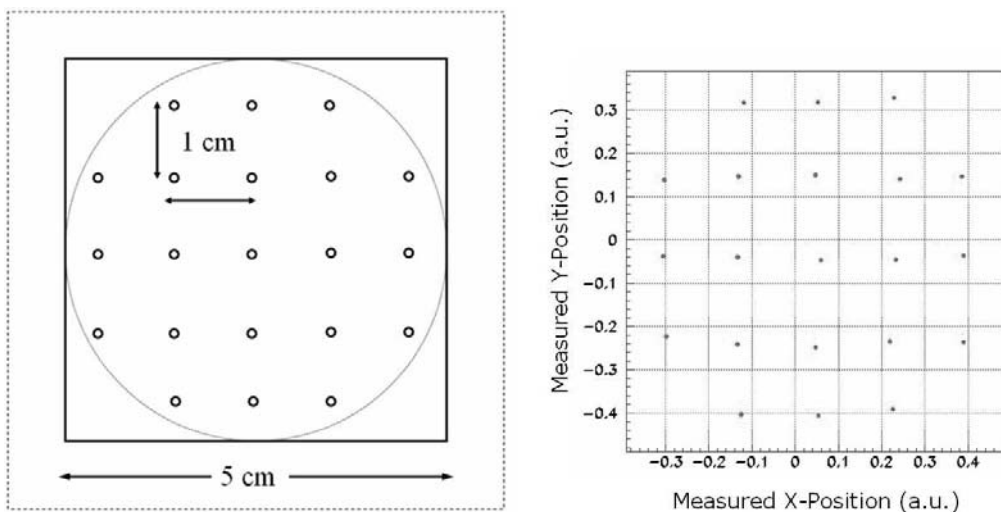


Figure 2. The geometry of the 21-hole matrix grid (left) used to calibrate the spatial information obtained from the PSPMT by applying light pulses and the reconstructed position diagram (right).

This experimental setup was used to calculate the intrinsic response and the spatial resolution of the PSPMT. Measured quantities were the accumulated charge  $Q$ , its spread  $\Delta Q$  at a given position  $(X, Y)$  of the PSPMT according to reconstruction Equations (1)–(3) and the spatial resolution  $\Delta X$  and  $\Delta Y$  obtained by performing a Gaussian fit to the

signal distribution around the point  $(X, Y)$ . The results are summarized in Figure 3 and Figure 4, where the High Voltage is operated in the range 850 V – 1150 V and the LED pulse duration in the range 200 ns – 1600 ns.

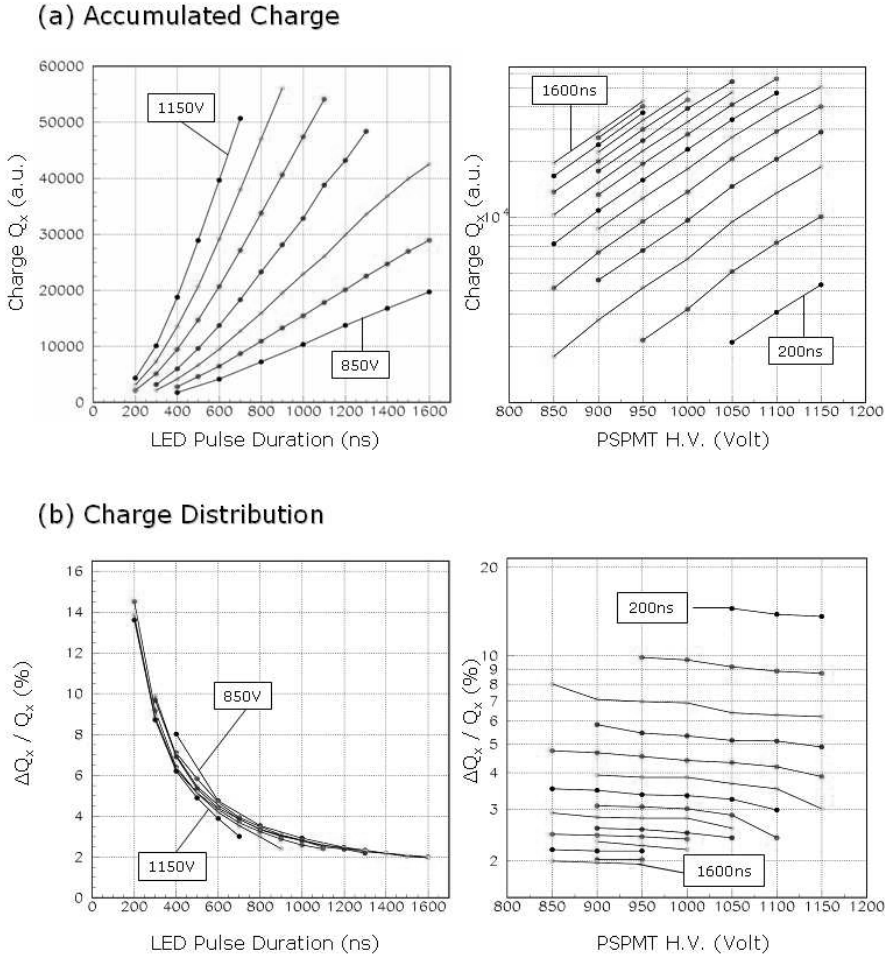


Figure 3. Accumulated charge  $Q$  and relative charge distribution  $\Delta Q/Q$  of the x-group wires of the PSPMT for the High Voltage operation range 850 V – 1150 V (in steps of 50 V) and LED pulse duration range 200 ns – 1600 ns (in steps of 100 ns). Similar curves are also obtained for the y-group wires.

In Figure 3 some of the most important features of the intrinsic response of the photomultiplier tube are exhibited. First, the linear response of the PSPMT i.e. the linear increase of the measured charge with the increase of the amount of light is obvious. Secondly, the logarithmic dependence of the accumulated charge on the high voltage is clearly shown, dependence that is expected considering the amplification procedure on

the PMT's dynode system. From the charge spread curves  $\Delta Q/Q$  it can be seen that the charge (energy) resolution doesn't depend on the High Voltage operation value since it remains practically constant for a given pulse width. The main dependence of the energy resolution is only on the pulse width and it is of exponential nature as shown in the same figure.

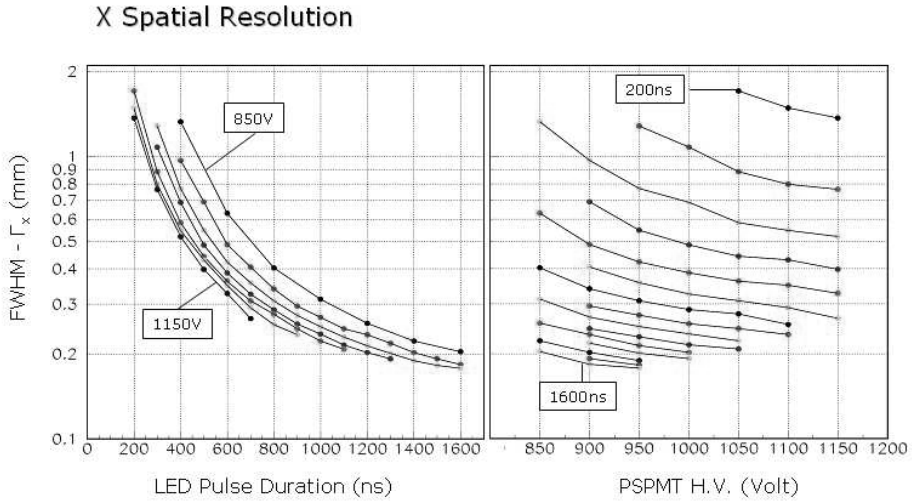


Figure 4. PSPMT's spatial resolution for the x-direction as a function of the High Voltage operation and the LED pulse duration (same ranges as in previous figure). Similar curves are also obtained for the y-direction.

In Figure 4 the PSPMT's spatial resolution for the x-direction as a function of the applied High Voltage and the LED pulse width is shown. It can be easily understood that the pulse width is proportional to the amount of optical light guided to the PSPMT and therefore a strong dependence of the spatial resolution on the pulse width is expected. It can be clearly seen from the graphs that increase of the pulse width leads to decrease of the FWHM-value i.e. to a better position resolution. From the same graphs one should also notice the weak dependence of the resolution on the High Voltage operation values. Similar curves are also obtained for the spatial resolution in the y-direction.

All the measurements of the previous graphs are referred to the central position of the photomultiplier tube. Nevertheless, a smooth deviation is expected for other coordinates and especially for the edge points of the effective field of view. For a given High Voltage operation value and a fixed LED pulse duration an average value from all measured 21 grid points can be performed. The spatial resolution values based on this method and obtained for High Voltage 850 V and pulse width  $1 \mu s$ :

$$\langle FWHM \rangle_x = (0.222 \pm 0.017) \text{ mm} \quad \langle FWHM \rangle_y = (0.233 \pm 0.016) \text{ mm}$$

indicate an upper limit in the spatial resolution which can be achieved for this  $\gamma$ -Camera system.

### 3.2. $\gamma$ -Camera System Resolution Study

In this final section results are presented for the complete  $\gamma$ -Camera system i.e. including the 4 mm pixelated CsI(Tl) crystal and the collimator. In order to measure the position resolution of the system a phantom was used, consisted of three capillaries (1.6 mm outer diameter) filled with water solution of  $^{99m}\text{Tc}$  (10 mCi/cm<sup>3</sup>). Three other empty capillaries were interposed in order to keep the filled ones in fixed relative distances. This asymmetric configuration 1-0-1-0-1 (0:empty, 1:filled) was placed in front of the collimator and data were recorded for several minutes (200,000 events). Measurements were performed for both horizontal and vertical phantom orientation.

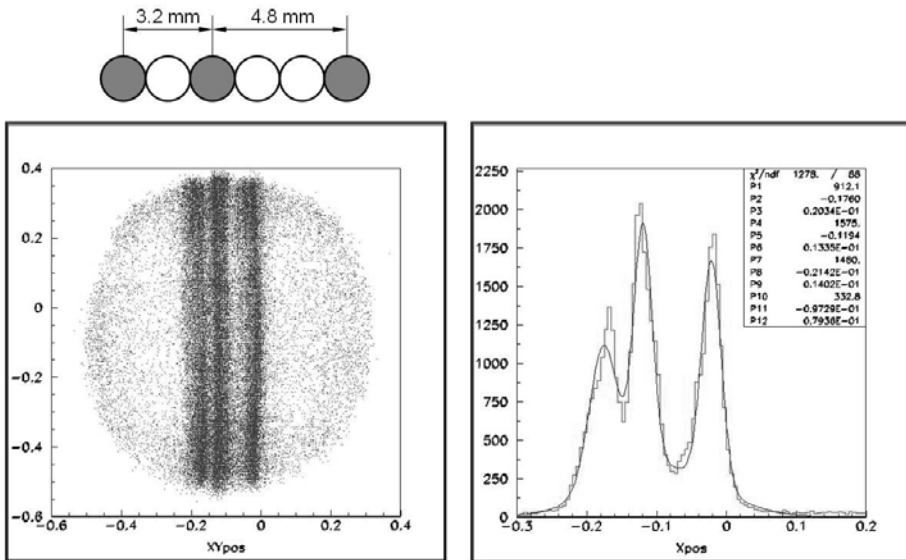


Figure 5. Planar image and its x-projection histogram of a phantom with 3 capillaries filled with  $^{99m}\text{Tc}$  water solution in a geometry indicated at the top of the figure.

The planar image obtained for the vertical phantom orientation is shown in Figure 5. The position resolution was calculated by fitting three Gaussian curves at the x-projection histogram. In a more precise way the vertical area was divided in uniform cuts and the procedure was repeatedly applied to all projections. Similar results for the horizontal phantom orientation obtained in complete analogy. The mean values for both orientations are:

$$\langle \sigma_x \rangle = (0.95 \pm 0.05) \text{ mm}$$

$$\langle \sigma_y \rangle = (1.07 \pm 0.07) \text{ mm}$$



#### 4. Conclusions and Future Plans

The intrinsic response and the resolution of the HAMAMATSU R2486 Position Sensitive PhotoMultiplier Tube has been extensively studied using the resistive chain technique and a Data Acquisition System based on PCI electronics. Dependencies of the accumulated charge, charge distribution and spatial resolution on High Voltage operation and incident light have been obtained. The PSPMT as well as the whole  $\gamma$ -Camera system shows a promising spatial and energy resolution.

A number of developments are under way. A collimator study based on GEANT4 and GATE simulations is being currently performed. In parallel, different types of scintillation materials are under investigation and there are plans for the systematic study of the system's response to several radiotracers.

This work is partially supported by the program PENED (03 E $\Delta$  287) of the General Secretariat for Research and Technology Hellas and by the program KAPODISTRIAS (Special Account for Research Grants) of the National and Kapodistrian University of Athens.

#### REFERENCES

1. H.O. Anger, *Scintillation Camera*, Rev. Sci. Instrum. **29** (1958) 27–33
2. R. Pani *et al.* *Scintillating array gamma camera for clinical use*, Nucl. Instrum. & Methods A **392** (1997) 295–298
3. J. Kim *et al.* *Development of a miniature scintillation camera using an NaI(Tl) scintillation and PSPMT for scintimammography*, Phys. Med. Biol. **45** (2000) 3481–3488
4. G.K. Loudos *et al.* *A 3D high-resolution gamma camera for radiopharmaceutical studies with small animals* Applied Radiation and Isotopes **58** (2003) 501–508
5. R. Pani *et al.* *A novel compact gamma camera based on flat panel PMT*, Nucl. Instrum. & Methods A **513** (2003) 36–41
6. F. Sánchez, J.M. Benlloch *et al.* *Design and test of a portable mini gamma camera* Med. Phys. **31** (2004) 1384–1397
7. H. Kim *et al.* *SemiSPECT: A small-animal single-photon emission computed tomography (SPECT) imager based on eight cadmium zinc telluride (CZT) detector arrays*, Med. Phys. **33** (2006) 465–474
8. V. Spanoudaki *et al.* *Design and development of a position-sensitive  $\gamma$ -Camera for SPECT imaging based on PCI electronics*, Nucl. Instrum. & Methods A **527** (2004) 151–156
9. V. Spanoudaki *et al.* *A  $\gamma$ -Camera System for SPECT Imaging based on PCI Electronics*, MSc Thesis, Physics Department, National and Kapodistrian University of Athens, 2003.
10. Hamamatsu Technical Data Sheet, *Position Sensitive Photomultiplier Tubes With Crossed Wired Anodes R2486 Series*, Hamamatsu Photonics, 1998.
11. ADLink Data Sheet, *PCI 9812/9810 20 MHz Simultaneous 4-CH Analog Inut Cards*, ADLink Technology, 2003.